

Phenothiazines solution complexity – determination of pK_a and solubility-pH profiles exhibiting sub-micellar aggregation at 25 and 37 °C

Aneta Pobudkowska ^{a,*}, Clara Ràfols ^b, Xavier Subirats ^b, Elisabeth Bosch ^b, Alex Avdeef ^c

^a Department of Physical Chemistry, Faculty of Chemistry, Warsaw University of Technology, Noakowskiego 3, 00-664 Warsaw, Poland;

^b Departament de Química Analítica and Institut de Biomedicina (IBUB), Universitat de Barcelona, Martí i Franquès 1-11, E-08028 Barcelona, Spain;

^c *in-ADME* Research, 1732 First Avenue #102, New York, NY 10128, USA.

* Corresponding author: Tel.: +48 22 234 74 75; fax: +48 22 628 27 41.

E-mail address: pobudka@ch.pw.edu.pl (A. Pobudkowska).

ABSTRACT

The ionization constants (pK_a) and the pH-dependent solubility ($\log S$ -pH) of six phenothiazine derivatives (promazine hydrochloride, chlorpromazine hydrochloride, triflupromazine hydrochloride, fluphenazine dihydrochloride, perphenazine free base, and trifluoperazine dihydrochloride) were determined at 25 and 37 °C. The pK_a values of these low-soluble surface active molecules were determined by the cosolvent method (*n*-propanol/water at 37 °C and methanol/water at 25 °C). The $\log S$ -pH profiles were measured at 24 h incubation time in 0.15 M phosphate buffers. The $\log S$ -pH “shape-template” method, which critically depends on accurate pK_a values (determined independently of solubility data), was used to propose speciation models, which were subsequently refined by rigorous mass-action weighted regression procedure described recently. Differential scanning calorimetry (DSC), UV-visible spectrophotometry, potentiometric, and high performance liquid chromatography (HPLC) measurements were used to characterize the compounds. The intrinsic solubility (S_0) values of the three least-soluble drugs (chlorpromazine·HCl, triflupromazine·HCl, and trifluoperazine·2HCl) at 25 °C were 0.5, 1.1, and 2.7 $\mu\text{g/mL}$ (resp.). These values increased to 5.5, 9.2, and 8.7 $\mu\text{g/mL}$ (resp.) at the physiological temperature. The enthalpies of solution for the latter compounds were exceptionally high positive (endothermic) values (99-152 $\text{kJ}\cdot\text{mol}^{-1}$). Cationic sub-micellar aggregates were evident (from the distortions in the $\log S$ -pH profiles) for chlorpromazine, fluphenazine, perphenazine, and trifluoperazine at 25 °C. The effects persisted at 37 °C for chlorpromazine and trifluoperazine. The solids in suspension were apparently amorphous in cases where the drugs were introduced as the chloride salts.

1. Introduction

Many surface-active ionizable drug molecules, especially those which are poorly soluble, exhibit complicated aqueous solution chemistry, in some ways like that of common detergents and bile salt surfactants. Dilute aqueous solutions of detergents (e.g., sodium dodecyl sulfate) consist of monomers located at the air-water interface. When the amount of the surfactant is increased past the critical micelle concentration (CMC), the monomer concentration becomes constant (at the CMC), as large water-soluble micelles (aggregation numbers ~ 50 , low polydispersity) form, accompanied by sharp transitions in many physical properties of the solution (Pramauro and Pelezetti, 1996; Ekwall, 1954; Fontell, 1971; Mukerjee and Cardinal, 1976; Chang and Cardinal, 1978).

Unlike that of the well-studied surfactants, the solution chemistry of low-soluble amphiphilic ionizable drugs is often associated with the formation of *sub-micellar* aggregates, with examples such as amiodarone (pentamer, $\text{pH} < 7$), hydralazine (hexamer, $\text{pH} < 7$), pramoxine (octamer, $\text{pH} < 8$) (Bouligand *et al.*, 1998; Bergström *et al.*, 2004), and prostaglandin $\text{F}_2\alpha$ (octamer, $\text{pH} > 5$) (Roseman and Yalkowsky, 1973). There are only a handful of other examples of sub-micellar aggregation (Higuchi *et al.*, 1953; Bogardus and Blackwood, 1979; Serajuddin and Rosoff, 1984; Serajuddin and Jarowski, 1985; Fini *et al.*, 1995; Zhu and Streng, 1996; Ledwidge and Corrigan, 1998; Jinno *et al.*, 2000). In the above examples, the stoichiometries of aggregation were estimated from the re-analysis of published solubility-pH data (Avdeef 2007, 2012; Völgyi *et al.*, 2013; Avdeef, 2014a,b; Butcher *et al.*, 2015).

The above drugs precipitate over a wide range of pH, forming solid phases in contact with dissolved monomers, and often, also with water-soluble sub-micellar aggregates (e.g., dimers, trimers ...), and in some cases, fully-formed micelles. Such aggregates are expected to have high solubility, strongly depend on temperature. Their solution behavior is poorly characterized and incompletely understood.

More recently, independent techniques have suggested the presence of sub-micellar

aggregates: Caco-2 permeability-pH data have been used to propose the presence of aggregated retinoic acid (Avdeef and Tam, 2010); ESI-Q-TOF-MS/MS was used to confirm the presence of dimers and trimers of cefadroxil in solution Shoghi *et al.* (2012).

Surface-active phenothiazines are prone to micelle formation. Attwood *et al.* (1974) found that distilled water solutions of promazine hydrochloride and chlorpromazine hydrochloride at 34 °C form small micelles, in aggregated units of eleven monomers, possessing eight units of net positive charge. Zografi and Zarenda (1966) noted that a 2-5 μM (below solubility limit) alkaline solution (pH 9-12) prepared from chlorpromazine *free base* showed no surface activity. However, 30 μM chlorpromazine *hydrochloride* at pH 9 produced stable supersaturated solutions, which partly separated as oil (liquid-liquid phase separation, LLPS) which was more soluble than the crystalline free base.

The aim of the present study was to characterize aqueous solubility-pH behavior of several poorly-soluble CNS-acting phenothiazine derivatives, including promazine·HCl, chlorpromazine·HCl, triflupromazine·HCl, fluphenazine·2HCl, perphenazine (free base), and trifluoperazine·2HCl. The phenothiazines belong to the neuroleptics class of drugs. They potently block dopamine receptors, and have been used for many years to treat the clinical symptoms of psychosis. Phenothiazines may also weakly interact with receptors 5-HT₂, effecting their antipsychotic activity. The substances can also inhibit neuroleptic receptors: histamine H₁, which is associated with sedation, and muscarinic M₁, which is responsible for symptoms such as memory impairment, drowsiness, and the antiemetic response (Patrick, 1995; Jaszczyszyn *et al.*, 2012).

Phenothiazine solubility was measured after 24 h in 0.15 M phosphate buffers in the pH interval from 6 to 11. The intent was to characterize the uncharged-drug precipitate region. However, some of the data revealed the presence of drug-phosphate salt precipitates in neutral solution. The ionization constants (pK_a), which are required for the interpretation of the solubility profiles, were measured by the cosolvent potentiometric and spectrophotometric methods. Both measurements were performed at 25 and 37 °C. Sub-micellar reactions were anticipated, given the surface activity of such compounds (Zografi *et al.*, 1964; Zografi and

Zarenda, 1966; Sorby *et al.*, 1966; Green, 1967; Florence and Parfitt, 1971; Attwood *et al.*, 1974; Liu and Hurwitz, 1977; Attwood *et al.*, 1997).

2. Materials and methods

2.1 Chemicals and reagents

The phenothiazine drugs (Figure 1) were obtained from Sigma Aldrich: promazine hydrochloride (CAS Registry No. 53-60-1), chlorpromazine hydrochloride (CAS Registry No. 69-09-0), triflupromazine hydrochloride (CAS Registry No. 1098-60-8), perphenazine free base (CAS Registry No. 58-39-9), fluphenazine dihydrochloride (CAS Registry No. 146-56-5), and trifluoperazine dihydrochloride (CAS Registry No. 440-14-5). The powders or small crystals were used as received, without further purification. Other chemicals used were as follows: *n*-propanol (*n*-PrOH) for cosolvent titrations (CAS Registry No. 71-23-8, Panreac, 99.5%), methanol (MeOH) for HPLC – super gradient (CAS Registry No. 67-56-1, POCH, 99.9%), hydrochloric acid (CAS Registry No. 7647-01-0, POCH, 35-38%), sodium hydroxide (CAS Registry No. 1310-73-2, POCH, 98.8%), potassium dihydrogen phosphate (CAS Registry No. 7778-77-0, POCH, 99.5%), dipotassium hydrogen phosphate (CAS Registry No. 7758-11-4, POCH, 99%), phosphoric acid (CAS Registry No. 7664-38-2, POCH, 85%), potassium hydroxide (CAS Registry No. 1310-58-3, POCH, 85%), disodium hydrogen phosphate (CAS Registry No. 7558-79-4, POCH, 99%), borax (CAS Registry No. 1303-96-4, POCH 99.5%), sodium chloride (CAS Registry No. 7647-14-5, POCH, 99.5%). Water was purified by the Milli-Q® plus system from Millipore (Billerica, MA, USA) with a resistivity of 18.2 MΩ·cm.

2.2 pK_a measurements

Preliminary pK_a values were determined at 25 °C by the traditional Bates-Schwarzenbach spectrophotometric method (Domańska *et al.*, 2009). However, some of the compounds proved to be difficult to characterize, since the method assumes that the Henderson-Hasselbalch equation is valid and that the sample remains fully dissolved during the

measurement.

Due to the very low solubility and surface activity of the phenothiazines, the pK_a values were also measured using purpose-built automated pK_a instruments, based on both potentiometric and spectrophotometric methods (Takács-Novák *et al.*, 2001; Völgyi *et al.*, 2007; Box *et al.*, 2007; Sun and Avdeef, 2011). Specifically, the pK_a values of fluphenazine·2HCl, perphenazine and trifluoperazine·HCl were assayed at 37 °C and $I = 0.15$ M by the following methods: (a) spectrophotometric in aqueous solution (D-PAS UV instrument, Sirius Analytical, UK), (b) potentiometric in aqueous solution (GLpKa instrument, Sirius Analytical, UK), and (c) potentiometric using *n*-PrOH as cosolvent, where blank titrations were performed using the particular solvent composition used later on the pK_a determination. In the latter method, densities at different cosolvent compositions, needed to define weight percentage (wt%), were obtained from the literature (Wohlfarth, 2008). Two series from 15 to 33 wt% *n*-PrOH were performed in two consecutive weeks.

At 37 °C, the use of methanol is not recommended, due to its high volatility; *n*-propanol is more suitable, having a vapor pressure comparable to that of water.

The same approach was tried with promazine·HCl, chlorpromazine·HCl, and triflupromazine·HCl at 37°C and $I = 0.15$ M. However, not all methods worked, due to extensive precipitation in alkaline solutions. Triflupromazine·HCl was evaluated at 25 °C and $I = 0.15$ M in MeOH cosolvent systems: potentiometrically (GLpKa) in the interval 34-64 wt% MeOH, and spectrophotometrically (D-PAS) in 5-52 wt% MeOH.

The pK_a values at 25 °C for chlorpromazine·HCl, promazine·HCl, fluphenazine·2HCl, perphenazine, and trifluoperazine·2HCl were taken from literature sources, determined by extrapolation from alcohol/water media (Avdeef, 1994, 2001; Shalaeva *et al.*, 2008; Tsinman *et al.*, 2010).

2.3 pH-Dependent solubility studies

The shake flask method was used to determine the solubility at 25 and 37 °C. Each drug was added in excess to 10 mL of 0.15 M KH_2PO_4 or K_2HPO_4 . The test tubes with the drug

suspensions were placed on a plate shaker. The solutions were thermostated (± 0.1 °C) using a circulating bath (Lauda A3, Germany). The pH of each solution was measured (CPC-401 ELMETRON, analytio GmbH, Germany, pH meter, ± 0.01 resolution), and adjusted as necessary, either with 0.1 M KOH or 0.1 M H₃PO₄, to the desired pH value. These values were re-checked at various times during the stirring. The experiment was completed when at least three pH measurements performed at an early, an intermediate and a late time-point of the 24 h period resulted in the same pH value. After 24 h, excess solid was separated using a rotating-bottle centrifuge at 5000 RPM for 20 min (Hettich Zenrifugen, EBA 20) or by filtration. The pH values were also measured of the supernatants, in order to verify that the drug solutions had the same pH value as the suspensions. The concentration of the drug in the supernatant solution was determined by an HPLC procedure with single-wavelength UV detection. All compounds were analysed in quadruplicate at each pH value.

2.4 HPLC analysis

Drug concentration in each sample was measured with HPLC-UV-vis apparatus, consisting of the 1200 Series Quat pump, vacuum degasser, and DAD/MWD (Agilent Technologies). A C18 analytical column (4.6 mm \times 150 mm) with a mean particle size of 5 μ m was used. Two solutions were used as a mobile phase: methanol (A) and phosphate buffer, pH = 7 (B). Injection volumes of 20 μ L were used during the analysis. The limit of detection (LOD) in the method used was <10 μ M. The chromatographic conditions for all the drugs are shown in Table 1.

2.5 Refinement of Intrinsic, Salt Solubility and Aggregation Constants

The solubility analysis, refinement, and simulation computer program, *pDISOL-X*TM (*in-ADME* Research), was used in this study. The mathematical approach in *pDISOL-X* has been described by Völgyi *et al.* (2013), and the program has been applied in several other recent studies (Avdeef, 2014a, b; Butcher *et al.*, 2015; Avdeef, 2015a). Briefly, the novel data analysis method uses solubility as a function of pH, log *S*-pH, as measured input data from any

analytical technique (along with standard deviations, $SD(\log S)$). The mass action algorithm considers the contribution of all species proposed to be present in solution, including all buffer components. The approach does not assume the validity of the Henderson-Hasselbalch (HH) relationship, nor does it depend on any explicitly derived extensions of the HH equations. The mass action algorithm derives its own implicit equations internally, given any practical number of reactions and estimated constants, which are subsequently refined by weighted nonlinear least-squares regression (Avdeef, 2012; Völgyi *et al.*, 2013). Therefore, in principal, drug-salt precipitates, -aggregates, -complexes, - bile salts, -surfactant can be evaluated. The presence of specific buffer-drug species can be tested. The program assumes an initial condition of a suspension of the solid drug in a solution, ideally with the suspension saturated over a wide range of pH. The program calculates the distribution of species consequent to a sequence of additions of standardized strong-acid titrant HCl (or ionizable-acid titrants H_3PO_4 , H_2SO_4 , acetic acid, maleic acid, lactic acid) to simulate the suspension pH-speciation down to $pH < 1$, the staging point for the subsequent operation. A sequence of perturbations with standardized strong-base titrant (e.g., NaOH) is simulated, and solubility calculated at each point (in pH steps of 0.005-0.2), until $pH > 12$ is reached. The ionic strength, I , is rigorously calculated at each step, and pK_a values (as well as solubility products, aggregation and complexation constants) are accordingly adjusted for changes in I from a benchmark level of 0.15 M (Avdeef, 1992, 2012).

At the end of the pH-speciation simulation, the calculated $\log S$ vs. pH curve is compared to measured $\log S$ vs. pH. A user-supervised $\log S$ -weighted nonlinear least squares refinement commences to refine the user-proposed solution model, using internally-derived analytical expressions for the differential equations. The process is repeated until the differences between calculated and measured $\log S$ values reach a minimum, as described elsewhere in detail.

2.6 Thermodynamics measurements

The temperature and enthalpy of fusion ($T_{\text{fus},1}$ and $\Delta_{\text{fus}}H_1$) and the temperature and enthalpy of solid–solid phase transition ($T_{\text{tr},1}$ and $\Delta_{\text{tr}}H_1$) were measured for the starting forms of the solids using a differential scanning microcalorimetry technique at the $5 \text{ K} \cdot \text{min}^{-1}$ scan rate with the power sensitivity of $16 \text{ mJ} \cdot \text{s}^{-1}$ and with the recorder sensitivity of 5 mV . The Perkin-Elmer Pyris 1 apparatus was calibrated with a 0.999999 mol fraction purity indium sample.

In addition, solids were separated from the suspensions by filtration after 24 hours near pH 7 and 10, where they were expected to be in the free-base form. The solids were rinsed and dried, after which DSC measurements were made.

3. Results and discussion

3.1 Ionic strength dependence of constants: pK_a , aggregation, solubility products

Table 2 indicates that some of the literature pK_a values were determined by capillary electrophoresis at ionic strength, $I = 0.05 \text{ M}$, whereas the rest of the pK_a values were determined near $I = 0.15 \text{ M}$. This is not problematic, since pK_a values of *monoprotic* bases are minimally affected by changes in the ionic strength in the $0.05 - 0.15 \text{ M}$ range.

However, the same is not so for the other constants (e.g., $2-pK_a$ bases, aggregation constants, solubility products). Ionic strength is not easily controlled in solubility-pH measurement, especially if the drug is introduced as a salt, or if highly-charged aggregates form, or if salts precipitate. Ionic strength can vary according to pH of the solution. Also, the use of 0.15 M phosphate buffer contributes to the total ionic strength. The ionic strength dependence of charged-species aggregation constants and solubility products can be substantial. In the current set of log S-pH measurements, the average ionic strength ranged from 0.32 to 0.36 M . Had we specifically intended to study the phosphate salt formation, then large sample weight would have been needed (cf., Sec. 3.3.10). To reach the point where phosphate salts of chlorpromazine, fluphenazine and trifluoperazine would have precipitated, the predicted ionic strength would have reached 1.6 M .

The *pDISOL-X* program is designed to make appropriate reconciliation for point-by-point

variation in ionic strength. A reference value, I_{ref} , is selected, typically set equal to the value of the mean ionic strength from the pK_a determination (e.g., 0.15 M). The constants in the solubility calculation are iteratively refined with respect to the fixed value of I_{ref} , but are continuously adjusted in the mass balance calculation to the variable ionic strength, I , for each value of pH. The procedure includes the calculation of the activity coefficients using hydration theory proposed by Stokes and Robinson (1948), and has been detailed elsewhere (Wang *et al.*, 2002; Völgyi *et al.*, 2013).

3.2 pK_a Determination

The results of the pK_a analysis are summarized in Table 2. Figure 2 shows the weighted linear regression cosolvent plots of the phenothiazines at 25 and 37 °C.

The measurement of the pK_a of many of the phenothiazines proved to be quite challenging, especially at 25 °C. It was found that the pK_a values estimated by the Bates-Schwarzenbach method were subject to systematic error, likely due to the formation of sub-micellar aggregates and precipitation at high pH with several of the drugs. For example, fluphenazine at 25 °C (Figure 3g) might appear to have a $pK_a = 8.73$ (rather than 7.84), were it not recognized that aggregates form.

The potentiometric pK_a measurements in aqueous solution were particularly problematic for chlorpromazine·HCl, promazine·HCl and triflupromazine·HCl due to their low solubility, even at 37 °C. In very dilute solution, it was possible to determine the pK_a of promazine·HCl spectrophotometrically. Some spectrophotometric titrations of chlorpromazine·HCl and triflupromazine·HCl had to be aborted because of precipitation at pH > 9.5. In those cases, final spectrophotometric pK_a values were calculated as the mean value of results from all titrations (from complete and aborted titration curves, but only when the number of experimental points before precipitation was sufficient for the determination).

The simultaneous determination of pK_{a1} and pK_{a2} of fluphenazine·2HCl, perphenazine, and trifluoperazine·2HCl from the whole titration data taken from single spectrophotometric experiments led to poor fittings for perphenazine and trifluoperazine·2HCl, but single pK_a

fittings (pK_{a1} or pK_{a2} separately) allowed a successful determinations. In the aqueous potentiometric determinations, only pK_{a1} was successfully determined, since the compounds precipitated at pH values close to pK_{a2} . The potentiometric *n*-PrOH/water method was successful in determining both of the pK_a values of the three piperazine derivatives at 37 °C.

Triflupromazine·HCl at 25 °C and $I = 0.15$ M was first studied in 34-64 wt% MeOH. Below 40 wt%, there were signs of some precipitation at elevated pH. The long-reach extrapolated pK_a was 9.58 ± 0.03 , almost identical to that of chlorpromazine·HCl. Subsequently, the spectrophotometric study was conducted to confirm this value. It was possible to work with significantly lower concentrations, thus extending the cosolvent range considerably, to 5 - 52 wt% MeOH. The extrapolated value was 9.49 ± 0.01 . It was decided to pool the data (37 individual titrations) into a single weighted linear regression analysis, which produced the final pK_a 9.47 ± 0.01 . The linearity of the plot in Figure 2e over the large range of MeOH/water ratios makes this pK_a value highly reliable.

The 25 °C promazine·HCl MeOH/water-extrapolated pK_a 9.62 ± 0.10 (Figure 2a) was based on the data from Shalaeva *et al.* (2008), determined by capillary electrophoresis (CE) at $I = 0.05$ M. The value is predicted to be 9.63 at $I = 0.15$ M (cf., Sec. 3.1). At 37 °C, the *n*-PrOH/water-extrapolated pK_a 9.11 ± 0.03 (Figure 2b) was accordingly lower than the room temperature value.

Chlorpromazine·HCl at 25 °C (Figure 2c) was an extrapolation from high MeOH/water ratios, to avoid precipitation and to minimize surface activity effects. Two sources of potentiometric (Avdeef, 1994, 2001) and CE (Shalaeva *et al.*, 2008) data were merged in the weighted linear regression analysis. Although the average ionic strength was 0.11 M, the measured pK_a corrected to $I = 0.15$ M (Sec. 3.1) remained essentially unchanged.

Generally, the two- pK_a piperazine-containing derivatives were less problematic to assess, especially at 37 °C, as illustrated in Figures 2g-2l. It is interesting that the lower pK_a value could be determined from cosolvent-*free* titrations. The direct measurements at zero cosolvent validated the extrapolation procedure from *n*-PrOH/water sets (Figures 2h, j, l). In retrospective, it may be that the 25 °C pK_{a1} (the lower pK_a) for trifluoperazine·2HCl (Tsinman *et*

al., 2011) could have been determined in cosolvent-free solution. The MeOH/water p_sK_{a1} values of that molecule indicated progressively higher errors with increasing amounts of methanol. This may be due to the decreased solubility of the dicationic salt in the organic solvent (Figure 2k).

It was apparent that the best overall results (gathered in Table 2) were those obtained by linear extrapolation of the apparent pK_a , p_sK_a , from *n*-PrOH/water (at 37 °C) and MeOH/water (at 25 °C) mixtures (p_sK_a vs. wt%) to zero cosolvent. These were better than those obtained by the Yasuda-Shedlovsky procedure, following the reasoning detailed elsewhere (Avdeef, 2012). The extrapolated values are very close of those obtained in aqueous solution by means of D-PAS instrument, where comparisons could be made.

3.3 Intrinsic solubility and sub-micellar speciation determination

Table 3 summarizes the results of the solubility-pH data analysis at 25 and 37 °C. (The units of the constants may be simply deduced by taking into account that all concentrations used in the analysis are based on molarity.) Each of the log S-H profiles is illustrated in Figure 3.

3.3.1 Henderson-Hasselbalch relationship

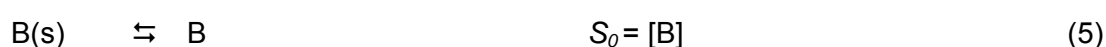
The dashed curves in Figure 3 were calculated with the Henderson-Hasselbalch (HH) equation, using the pK_a values from Table 2 and the intrinsic solubility values from Table 3. In the curves, the region for $pH \gg pK_a$ has zero limiting slope and the region for $pH \ll pK_a$ has a limiting slope of -1 (or -2 for $pH \ll pK_{a1}$ in the 2- pK_a piperazine derivatives). The measured log S values (solid circles) can deviate from the HH curves when (a) drug salts precipitate, (b) water-soluble aggregates form, (c) solutions remain substantially supersaturated, (d) LLPS oils or “drug-rich” particulates (Indulkar *et al.*, 2015) separate, (e) amorphous solids form to differing extents as a function of pH, or (f) when the analytical method reaches its limit of detection.

3.3.2 Solution chemistry model construction – “Shape Templates”

The solid lines in Figure 3 are best-fit curves through the measured log *S* values, calculated from the mass balance equations corresponding to the refined constants for the proposed reactions (below). A step-by-step solubility model construction (for a case similar to that of fluphenazine, Figure 3g) was described recently (Avdeef, 2014a). Each of the log *S*-pH profile shapes in Figure 3 was compared against a series of *templates* (Avdeef, 2007, 2012). For example, if the apparent slope in the log *S*-pH profile for pH < *pK_a* is -2 rather than -1 (as expected for one-*pK_a* derivatives), then a dicationic dimer, B₂H₂²⁺, may be indicated (Case 2b: Avdeef, 2007). A slope of -3 would suggest the presence of a trimer, and so on. However, if the slope is the normal -1, but the log *S*-pH curve as a whole is shifted to higher pH (appearing to indicate a higher *pK_a* than that measured independently), then a “half” charged aggregate, (B₂H⁺)_n, may be indicated (Case 3b: Butcher *et al.*, 2015). In the study here, numerous species were tested against the data, but only dimeric species were needed to rationalize the aggregation data region (pH > 6). This templating process requires knowing the accurate *pK_a*, independently determined under conditions where precipitation and aggregation are absent (Butcher *et al.*, 2015).

3.3.3 Model reactions and constants

The following reactions proved to be in best agreement with the data (not all for each drug). As a generalized example of a monoprotic weak base, B, a saturated solution can be defined by the equations and the corresponding reaction quotients:



The solubility of a drug substance at a particular pH is defined as the mass balance sum of the concentrations of all of the species dissolved in the aqueous phase, adjusted for the degree of aggregation:

$$\begin{aligned}
 S &= [B] + [BH^+] + 2 [B_2H_2^{2+}] + 2 [B_2H^+] + 2 [B_2] \\
 &= [B] + [H^+][B] / K_a + 2 K_2^{B_2H_2} [H^+]^2[B]^2 / K_a^2 + 2 K_2^{B_2H} [H^+][B]^2 / K_a + 2 K_2^{B_2} [B]^2 \quad (8)
 \end{aligned}$$

where the square brackets denote molar concentration of species.

It may be noted that in the full log S-pH profile (consisting of free base and salt precipitation), the pH point of discontinuity (e.g., pH 7.8 for promazine, Figure 3a), where the drug salt solubility portion of the curve intersects that of the free base, is called pK_a^{Gibbs} , a term introduced by Avdeef (1998), and further elaborated by Streng (1999). In the literature, this point is sometimes called “pH_{max}”, suggesting that the solubility reaches its maximum value at that point. However, the latter term is not general, since it has been shown that the intersection point may occur at solubility well below the maximum value, as in the examples of drug phosphate salts of verapamil, carvedilol, mifepristone, cyproheptadine, and thioridazine (Avdeef, 2014b).

Eq. (8) may be further transformed to contain only constants and $[H^+]$ (as the only variable). For $pH > pK_a^{\text{Gibbs}}$, where the free base is the sole precipitate, $[B]$ becomes constant, denoted as S_0 (“intrinsic” solubility). On factoring $[B]$ out of the second line of Eq. (8) and expressing the equation in logarithmic form, one gets

$$\begin{aligned}
 \log S &= \log S_0 + \log (1 + [H^+]/K_a + 2 S_0 \{ K_2^{B_2H_2} [H^+]^2/K_a^2 + K_2^{B_2H} [H^+]/K_a + K_2^{B_2} \}) \\
 &= \log S_0 + \log \left(\left\{ 1 + 10^{+pK_a - pH} + 2S_0 \cdot \right. \right. \\
 &\quad \left. \left. \left\{ 10^{+\log K_2^{B_2H_2} + 2pK_a - 2pH} + 10^{+\log K_2^{B_2H} + pK_a - pH} + 10^{+\log K_2^{B_2}} \right\} \right\} \right) \quad (9)
 \end{aligned}$$

If the solubility measurements were carried out in an acidic solution ($\text{pH} < pK_a^{\text{Gibbs}}$), with enough compound added that the solubility products $[\text{BH}^+]^2 [\text{HPO}_4^{2-}]$ and/or $[\text{BH}^+] [\text{H}_2\text{PO}_4^-]$ are exceeded, then Eq. (8) would be cast in terms of $[\text{BH}^+]$ being constant rather than $[\text{B}]$, and S_0 being replaced with the solubility product expression(s).

With the 2- pK_a drugs, one would also need to expand Eqs. (1)-(7) accordingly, and consider the additional possible solubility products: $[\text{BH}_2^{2+}][\text{H}_2\text{PO}_4^-]^2$, $[\text{BH}_2^{2+}][\text{HPO}_4^{2-}]$, $[\text{BH}_2^{2+}][\text{Cl}^-][\text{H}_2\text{PO}_4^-]$, etc., which would make Eqs. (8) and (9) further complicated. The low-pH ($< pK_{a1}$) data (if enough compound were added to exceed the above solubility products) could be quite complex and challenging to interpret for all the possible diprotic-drug phosphate salt formations. This low pH region was beyond the scope of the present study.

All such complex equations are sorted out implicitly in the mass action algorithm of *pDISOL-X*, and their explicit derivations are not necessary.

3.3.4 Promazine hydrochloride

In the free-base precipitation region, the promazine·HCl profile showed near adherence to the expected HH shape (Figures 3a, b). Below pH 7.7, promazine at 25 and 37 °C showed signs of 2:1 drug phosphate precipitation. To describe such processes, Eq. (6) needs to be considered. In the 2:1 salt solubility region where $\text{pH} < pK_a^{\text{Gibbs}}$, Eq. (8) still holds, but $[\text{BH}^+]$ becomes constant, instead of $[\text{B}]$. Eq. (9) can be modified to reflect this, as described in detail elsewhere (Avdeef, 2012; Völgyi *et al.*, 2013).

3.3.5 Chlorpromazine hydrochloride

Chlorpromazine·HCl is the most insoluble derivative considered here. Below pH 8, there is deviation from the HH form, consistent with the formation of dicationic dimers (Figure 3c,d). The three points at the lowest pH at 25 °C may indicate some supersaturation (Serajuddin and Rosoff, 1984; Serajuddin and Jarowski, 1985). It is noteworthy that the sub-micellar aggregates compete with the formation of phosphate salts. Concentrations of chlorpromazine

at 37 °C (Figures 3d) would need to be greater than 1 M before drug-phosphate salts would be expected to precipitate, due to the presence of stable $B_2H_2^{2+}$ dimers depleting the BH^+ species needed in the precipitate. There is substantial uncertainty in this prediction, due to the presence of the charged dimers.

3.3.6 Triflupromazine hydrochloride

As with chlorpromazine·HCl, triflupromazine·HCl may indicate some supersaturation below pH 7 at 25 °C (Figure 3e). As a departure from HH form, the most prominent feature in the log S-pH profile at 25 °C is the levelling off of points above pH 9, which may indicate the formation of water-soluble uncharged B_n aggregates (Case 1b: Avdeef, 2007). The value of n cannot be determined from pH dependence; $n = 2$ (cf., Eq. 4) was used for the refined constant (Table 3). Alternative explanations for the effect above pH 9 may be that (a) the solutions still remained supersaturated at the end of 24 h incubation time, or (b) partial LLPS oil separation persisted at the end of 24 h, or (c) the solid was amorphous preferentially in alkaline suspensions at the end of 24 h, or (d) simply that the analytical method reached its limit of detection. Nine compounds out of 25 bases were found (Avdeef, 2014b) to show this effect in the study of Bergström *et al.* (2004). Additional investigation is needed to better understand the nature of the non-HH behavior in basic solution.

3.3.7 Fluphenazine dihydrochloride

Fluphenazine·2HCl at 25 °C departed from HH form (Figure 3g), with a half-charged aggregate, $(B_2H^+)_n$, indicated (Case 3b: Butcher *et al.*, 2015). It is not possible to determine the aggregation number from pH dependence alone, so $n=1$ (i.e., species B_2H^+) was selected in the refinement of the dimer constant. The effect is less prominent at the higher temperature (Table 3).

It is noteworthy that the stable half-charged aggregate at 25 °C is expected to compete with the formation of phosphate salts by diminishing the formation of the BH^+ species, thus raising the predicted salt solubility (see below) to about 240 mg·mL⁻¹ below pH 5 (Figure 3g).

Experimental data below pH 7 are needed to further understand this largely uncharted Case 3b phenomenon, as the predictions are expected to be substantially uncertain there.

Lower salt solubility is predicted at 37 °C, compared to 25 °C, since the half-charged aggregate is weaker. The predicted (cf., Sec. 3.3.10) step discontinuity near pH 5.6 in Figure 3h marks the transition across the pK_a^{Gibbs} . At pH 5.1, the solid is predicted to be $\text{BH}\cdot\text{H}_2\text{PO}_4(\text{s})$. However, at pH 5.5, two solids are predicted to co-precipitate: $\text{BH}\cdot\text{H}_2\text{PO}_4(\text{s})$ and $(\text{BH})_2\cdot\text{HPO}_4(\text{s})$ at the salt pK_a^{Gibbs} . Above pH 5.6, only the B(s) solid is present in the saturated solution.

3.3.8 Perphenazine

Perphenazine (Figures 3i,j), the only phenothiazine introduced as a free base, appears to show only a small amount of aggregation. At 25 °C, Case 1b and 2b aggregates best rationalize the data. At 37 °C, the best fit of the data is with a Case 3b aggregate.

3.3.9 Trifluoperazine dihydrochloride

Trifluoperazine·2HCl shows substantial aggregation at both temperatures (Figure 3k,l). When drug phosphate salts are included in the model (see below), all solid is predicted to dissolve below pH 5 up to about 1 M added compound. The presence of the dicationic dimers is predicted to elevate salt solubility above 240 mg·mL⁻¹. The levelling off of data at 25 °C for pH > 8 may have similar interpretations as that of triflupromazine at 25 °C.

3.3.10 Prediction of phosphate salt solubility products

The *pDISOL-X* analysis of twenty-five low-soluble one- pK_a bases (Avdeef, 2014b), using log S-pH measurements in 0.15 M phosphate buffer (Bergström *et al.*, 2004), revealed correlations between the intrinsic solubility and the two phosphate solubility products:

$$\log K_{\text{sp}}^{2:1} = -0.76 + 1.20 \log S_0 \quad (10)$$

$$\log K_{\text{sp}}^{1:1} = -0.53 + 0.55 \log S_0 \quad (11)$$

These novel solubility product prediction equations were applied to the phenothiazines (cf., Table 3). The dash-dot curves in Figure 3 are based on the predictions. The agreement between prediction and measurement was good for promazine·HCl at both temperatures, and fair in the case of triflupromazine at 37 °C.

Eqs. (10) and (11) could be useful in planning experimental conditions for future studies dedicated to characterizing the phosphate solubility products of the drugs. They are used here mainly as guides of what to expect for pH < 6 profiles, where drug-phosphate salts are expected to form. Eqs. (10) and (11) would not apply to the 2- pK_a molecules in the low-pH (< pK_{a1}) regions, as noted earlier.

3.4 Phenothiazine thermodynamics

The differential scanning calorimetry (DSC) thermograms in Figure 4 confirm the polymorphic homogeneity of most of the solid samples. The dotted curves correspond to the starting forms of the solids used (mostly mono- or dihydrochloride, with one free base). The dashed curves correspond to solids isolated from solutions near pH 7, at the 24 h time points. The solid curves refer to those of the substances isolated near pH 10 at 24 h.

The DSC was used to determine the melting points and enthalpies of fusion (mostly of chloride salts), as summarized in Table 4. Only fluphenazine·2HCl indicated a solid-solid phase transition temperature (215.8 °C / 488.9 K). Perphenazine, being a free base, showed the lowest melting point (96.8 °C / 370.0 K) of the compounds studied. The melting enthalpy values range from 35.0 kJ·mol⁻¹ (promazine·HCl) to 64.5 kJ·mol⁻¹ (triflupromazine·HCl), and are typical values for organic compounds. The highest value of the enthalpy of melting (triflupromazine HCl) was concomitant to the decomposition of the substance.

The determination of log S_0 at two temperatures allowed for the calculation of the enthalpy of solution, using the van't Hoff equation,

$$\log S_2 = \log S_1 - \frac{\Delta H_{sol}^0}{2.303R} \cdot \left(\frac{1}{T_2} - \frac{1}{T_1} \right) \quad (12)$$

where $R = 8.3143 \text{ J}\cdot\text{mol}^{-1}$, $T_1 = 298.15$, and $T_2 = 310.15 \text{ K}$. The calculated values (Table 4) are all positive, indicative of an endothermic dissolution process. The three least soluble drugs have the highest heats of dissolution: $\Delta H_{\text{sol}}^0 = 152, 134, 99 \text{ kJ}\cdot\text{mol}^{-1}$ for chlorpromazine, triflupromazine, and trifluoperazine, respectively. The last column in Table 4 lists the predicted values of enthalpy of solution, based on a multiple linear regression model, trained with 626 molecules (Avdeef, 2015b). It is interesting to note that the above three least-soluble phenothiazines have the highest discrepancies between measured and calculated enthalpies. On the other hand, the agreement between the calculated and measured enthalpies of solution for the three most-soluble molecules is within the experimental uncertainties in such measurements (Avdeef, 2014b). It may be that the sub-micellar aggregation with the least-soluble molecules has an impact on the heats of dissolution based on the two-temperature results reported here. This is consistent with observations of others, that the solubility of drugs prone to the forming aggregates can be strongly dependent on temperature (Bogardus and Blackwood, 1979).

3.5 Solid form isolated from suspensions

The melting points reported in the literature for free-base phenothiazine derivatives are low: $25 \text{ }^\circ\text{C}$ for trifluoperazine and triflupromazine, $33 \text{ }^\circ\text{C}$ for promazine, $57 \text{ }^\circ\text{C}$ for chlorpromazine, and $96.8 \text{ }^\circ\text{C}$ for perphenazine (Bradley *et al.*, 2016). At the 24 h incubation time point, the solids isolated from the suspensions in this study did not appear to be oils by visual inspection. However, the calorimetric data were not straight forward to interpret. The DSC of solids separated from suspensions near pH 7 (dashed curves in Fig. 4) were largely featureless, possibly suggesting the presence of amorphous solids. This was the pH region where the solid was expected to be the free base form. The neutral pH region may be prone to supersaturation, more so than the pH 10 region. It was surprising that the drug substance isolated from pH 10 suspensions (solid curves in Fig. 4) showed sharp negative peaks in the DSC, corresponding to the starting *salt forms* of the solids (with the exception of

perphenazine), persistently 1-2 °C lower than those of the starting material (dotted curves in Fig. 4). The reasonable explanation for this is as follows. When the excess salt forms of the drugs were added to the buffer solutions at the low-pH end of the range selected and the pH values were adjusted with 0.1M KOH, the surfaces of the solids became covered with the free base which forms. (In the 37 °C solubility experiments, the free base may have been oil for some of the derivatives.) The encased drug chloride salts apparently become insulated from the aqueous phase. The free-base coating established an *apparent equilibrium* with the aqueous phase. This happens in rotating-disk dissolution studies, where hydrochloride salts of weak-base drugs dissolve quickly but then re-precipitate in the pH 6.8 phosphate buffer media as free bases on the surface of the dissolving rotating drug salt pellet (e.g., as shown visually for papaverine in Fig. 4 in Avdeef and Tsinman, 2008). This would not happen with perphenazine, since it had been introduced as a free base (cf., Fig. 4e), given that the observed melting point is identical to the literature value for the free base. If the coating on the surface of incompletely dissolved salt particles were the free base in crystalline form, then a DSC scan at low temperature might have partially revealed the expected low melting points. However, the DSC scan from 0 – 220 °C for promazine isolated from pH 10 suspension (Fig. 4a) shows a featureless plot near the expected 25 °C melting point region. The tentative conclusion is that the solid materials in our solubility studies were largely if not entirely amorphous, with the exception of perphenazine. Clearly, the solid state characterization is not complete and will require further detailed study, at longer incubation times than the 24 h in present study.

The “salt particles coated with free base” effect can be easily eliminated by (a) selecting a lower pH buffer (pH < 6) into which the salt is initially added, and (b) by using a smaller excess of salt to add to the buffer. Once the salt *completely dissolves*, additions of NaOH can commence to elevate the pH so free-base precipitates can form (free of entrapped salt). This was demonstrated with chlorpromazine hydrochloride, where the recovered solid base from the pH 10 solution showed the expected 57 °C melting point by DSC (data not shown).

3.6 Solid form introduced can influence supersaturation at pH near the pK_a^{Gibbs}

Zografi and Zarenda (1966) noted that chlorpromazine added to distilled water as the hydrochloride salt showed surface activity, but not when introduced as the free base. This could be due to the starting pH of the saturated water solutions. Since perphenazine was the only drug introduced as the free base in the present study, and since it showed a lesser tendency to form aggregates, compare to the other derivatives, it is useful to take note of the impact of the solid form introduced to solution on the presence/persistence of aggregates. Serajuddin and Mufson (1985) determined the log S-pH profiles of tiaramide at 1-2 h time points by introducing the free base or the hydrochloride form of compound. The pH region near the pK_a^{Gibbs} showed a strong tendency for supersaturation, *regardless* of the initial solid form of the drug. The same was so of the apparent cationic tetramer of tiaramide formed in the pH 4-5 interval. It was not reported how long the apparent aggregate persisted, since the system at 1-2 h may not have reached a steady state. Other drugs, studied over longer times, showed a similar tendency to supersaturate near the pK_a^{Gibbs} region of pH, often accompanied by the formation of aggregates on the free-base/acid side of the profile (Serajuddin and Rosoff, 1984; Serajuddin and Jarowski, 1985; Ledwidge and Corrigan, 1998; Li *et al.* 2005a, b). As far as we are aware, there have not been reported studies of the stability of the sub-micellar aggregates, although it is thought that supersaturation is time dependent.

3.7 Implications of sub-micellar aggregation

The last column in Table 3 lists the literature values of the phenothiazine CMC in acidic (pH 2) and phosphate-buffered (pH 6.9) solutions. The reported CMC of trifluoperazine and chlorpromazine in the pH 6.9 phosphate buffer at 25 °C are 37 and 150 μ M, respectively. The log S-pH profiles of chlorpromazine and trifluoperazine (Figures 3c,k) indicate a sub-micellar aggregates at concentrations *above* the reported CMC (Zografi *et al.*, 1964).

Ottaviani *et al.* (2015) considered the practical importance of CMC values of drugs. They found that in biorelevant media (e.g., bile salts), CMC values better correlated with the

solubility enhancement effect than did traditional lipophilicity descriptors (i.e., octanol-water partition coefficients). More complete knowledge of the sub-micellar aggregation property of candidate molecules could impact on formulation decisions, e.g., based on biorelevant media studies, and in the design and interpretation of salt selection investigations (Casares *et al.*, 2015).

3.8 Comparison of intrinsic solubility to literature values

A thorough search of the literature revealed multiple sources of intrinsic solubility values for all of the phenothiazines studied here. Almost all values were reported near room temperature (20-25 °C), with the exception of fluphenazine, which was only available at 37 °C. Table 5 summarizes the comparisons and Figure 5 displays the correlation between the values reported here and the averaged values from the literature. Before averaging the room temperature results, all room temperature values were transformed to a common 25 °C basis using a recently described procedure (Avdeef, 2015b), to match the temperature in the study here.

Figure 5 shows nearly perfect agreement for fluphenazine, promazine, and triflupromazine. For the other three compounds, the values reported here are up to 0.5 log units *lower* than the average values reported in the literature. This is an important observation.

Since our solid state characterization suggested the possibility of amorphous character to the solids isolated at the end of 24 h incubation times, it was of interest to estimate how far we may have been from the crystalline solid state (as a measure of equilibration). We selected 24 h as the incubation time based on constancy of concentrations rather than the presence of crystalline solids. It is noteworthy that in some of the literature methods (Table 5) incubation times of 24, 48, and 72 h were employed. It is frequently suggested that solubility values of amorphous solids are expected to be higher than that of crystalline solids. If our results were typical of amorphous solids, then all of the points in Figure 5 should have been *above* the identity line. *That is not what is indicated in Figure 5.* We thus propose that our reported values at the end of 24 h incubation are indistinct from those expected of values at true

chemical equilibrium.

4. Conclusions

For the six phenothiazines studied here, it was possible to rationalize the complex log S-pH profiles measured in 0.15 M phosphate buffer at 25 and 37 °C in the pH 6-11 region. This was so because highly reliable pK_a values became available, determined independently of the solubility data, under optimized conditions designed to avoid precipitation and sub-micellar aggregation. A state-of-the-art mass action computational algorithm was used to interpret the solubility data. Positively-charged sub-micellar aggregates were evident for chlorpromazine, fluphenazine, perphenazine, and trifluoperazine at 25 °C. The effects persisted at 37 °C for chlorpromazine and trifluoperazine. The presence of such aggregates may have been anticipated by the known surface-active behavior of the phenothiazines (e.g., very low CMC values in buffered solutions). The solution model developed here could be applied to fine-tune salt selection procedures of surface active molecules, and is expected to be useful in predicting to what extent solubility enhancement may be achieved by using biorelevant media. The DSC characterization suggested the presence of some amorphous form of solid in suspensions at the 24 h incubation time in cases where the drug was introduced as a chloride salt. Perphenazine, introduced as a free base, appeared to be crystalline when isolated from alkaline solution. Based on the comparison between the intrinsic solubility values reported here and the twenty-two values taken from the literature, we conclude that the 24 h incubation reached a state that may be indistinguishable from thermodynamic equilibration, within the bounds of experimental error, even though some of our solid state characterizations suggested the presence of amorphous solids. This will be further investigated in future studies by using solely free base phenothiazines as starting forms of solids.

Acknowledgements

Funding for some of this research was provided by the Warsaw University of Technology,

Warsaw, Poland. The authors from the University of Barcelona are grateful for the financial support of the Spanish government (Project CTQ2014-56253-R). We thank Marina Shalaeva of Pfizer, Groton, USA, for providing additional details concerning published pK_a determinations by capillary electrophoresis. We thank Abu Serajuddin and Ankita Shah of St. John's University (Queens, NY) for their insight into the interpretation of DSC characterizations.

REFERENCES

- Attwood, D., Florence, A.T, Gillan, J.M.N., 1974. Micellar properties of drugs: properties of micellar aggregates of phenothiazines and their aqueous solutions. *J. Pharm. Sci.* 63, 988-993.
- Attwood, D., Boitard, E., Dubès, J.-P., Tachoire, H., 1997. Calorimetric study of the influence of electrolyte on the micellization of phenothiazine drugs in aqueous solution. *J. Phys. Chem. B* 101, 9586-9592.
- Avdeef, A., 1992. pH-metric log P. 2. Refinement of partition coefficients and ionization constants of multiprotic substances. *J. Pharm. Sci.* 82, 183-190.
- Avdeef, A., 1994. Sirius Technical Application Notes (STAN). Vol. 1. Sirius Analytical Instruments Ltd.: Forest Row, UK.
- Avdeef, A., 1998. pH-metric solubility. 1. Solubility-pH profiles from Bjerrum plots. Gibbs buffer and pK_a in the solid state. *Pharm. Pharmacol. Commun.* 4, 165-178.
- Avdeef, A., 2001. High-throughput measurements of solubility profiles. In: Testa, B.; van de Waterbeemd, H.; Folkers, G.; Guy, R. (Eds.). *Pharmacokinetic Optimization in Drug Research*, Verlag Helvetica Chimica Acta: Zürich and Wiley - VCH: Weinheim, pp. 305-326.
- Avdeef, A., 2003. *Absorption and Drug Development, Solubility, Permeability and Charge State*, Wiley-Interscience, New York.
- Avdeef, A., Voloboy, D., Foreman, A., 2007. Dissolution – Solubility: pH, Buffer, Salt, Dual-Solid, and Aggregation Effects, in: B. Testa, H. van de Waterbeemd (Eds.). *Comprehensive Medicinal Chemistry II, Vol. 5 ADME-TOX Approaches*. Elsevier, Oxford, UK.
- Avdeef, A., Tsinman, O., 2008. Miniaturized rotating disk intrinsic dissolution rate measurement: effects of buffer capacity in comparisons to traditional Wood's apparatus. *Pharm. Res.* 25, 2613-2627
- Avdeef, A., 2007. Solubility of sparingly-soluble drugs. *Adv. Drug Deliv. Rev.* 59, 568-590.
- Avdeef, A., Tam, K.Y., 2010. How well can the Caco-2/MDCK models predict effective human jejunal permeability? *J. Med. Chem.* 53, 3566-3584.
- Avdeef, A., 2012. *Absorption and Drug Development Second Edition*, Wiley-Interscience, Hoboken NJ.

- Avdeef, A., 2014a. Anomalous Solubility Behavior of Several Acidic Drugs. *ADMET & DMPK* 2, 33-42.
- Avdeef, A., 2014b. Phosphate Precipitates and Water-Soluble Aggregates in Re-examined Solubility-pH Data of Twenty-five Basic Drugs. *ADMET & DMPK* 2, 43-55.
- Avdeef, A., 2015a. Suggested improvements for measurement of equilibrium solubility-pH of ionizable drugs. *ADMET & DMPK* 3, 84-109.
- Avdeef, A., 2015b. Solubility temperature dependence predicted from 2D structure. *ADMET & DMPK* 3, 298-344.
- Barton, A.F.M., 1985. *Solubility Parameters*. CRC Press, Boca Raton.
- Bates, R.G., Gary, R., 1961. Acidity functions. Values of the quantity $p(\alpha_{HYCl})$ for buffer solutions from 0 to 95 C. *J. Res. NBS* 65A, 495-505.
- Bergström, C.A.S., Norinder, U., Luthman, K., Artursson, P., 2002. Experimental and computational screening models for prediction of aqueous drug solubility. *Pharm. Res.* 19, 182-188.
- Bergström, C.A.S., Luthman, K., Artursson, P., 2004. Accuracy of calculated pH-dependent aqueous drug solubility, *Eur. J. Pharm. Sci.* 22, 387-398.
- Bogardus, J.B., Blackwood, R.K. Jr., 1979. Solubility of doxycycline in aqueous solution. *J. Pharm. Sci.* 68, 188-194.
- Bouligand, Y., Boury, F., Devoisselle, J.-M., Fortune, R., Gautier, J.-C., Girard, D., Maillol, H., Proust, J.-E., 1998. Ligand crystals and colloids in water-amiodarone systems. *Langmuir* 14, 542-546.
- Box, K.J., Völgyi, G., Ruiz, R., Comer, J.E., Takács-Novák, K., Bosch, E., Ràfols, C., Rosés, M., 2007. Physicochemical properties of a new multicomponent cosolvent system for the pK_a determination of poorly soluble pharmaceutical compounds. *Helv. Chim. Acta* 90, 1538-1553.
- Bardley, J.-C., Williams, A., Lang A. Jean-Claude Bradley Open Melting Point Dataset - Version 2. <http://www.chemspider.com/DatasourceDetails.aspx?id=800>, accessed 21 Feb 2016.
- Butcher, G., Comer, J., Avdeef, A., 2015. pK_a -critical Interpretations of solubility-pH profiles: PG-300995 and NSC-639829 case studies. *ADMET & DMPK* 3, 131-140.
- Casares, A.F, Nap, W.M., Figás, G.T., Huizenga, P., Groot, R., Hoffmann, M., 2015. An evaluation of salt screening methodologies. *J. Pharm. Pharmacol.* 67, 812-822.
- Chang, Y, Cardinal, J.R., 1978. Light-scattering studies on bile acid salts. I: Pattern of self-association of sodium cholate, sodium glycocholate, and sodium taurocholate in aqueous electrolyte solutions. *J. Pharm. Sci.* 67, 174-181.
- Domańska, U., Pobudkowska, A., Pelczarska, A., Gierycz, P., 2009. pK_a and solubility of drugs in water, ethanol, and 1-octanol. *J. Phys. Chem. B* 111, 8941-8947
- Ekwall, P., 1954. Concentration limits in association colloid solutions. *J. Colloid. Sci.* 9, Suppl. 1, 66-80.

- Fini, A., Fazio, G., Feroci, G., 1995. Solubility and solubilization properties of non-steroidal antiinflammatory drugs. *Int. J. Pharm.* 126, 95-102.
- Florence, A.T., Parfitt, R.T., 1971. Micelle formation by some phenothiazine derivatives. II. Nuclear magnetic resonance studies in deuterium oxide. *J. Phys. Chem.* 76, 3554-3560.
- Fontell, K., 1971. Micellar behavior in solutions of bile-acid salts. I. Vapor pressure of the aqueous solutions and the osmotic activity of the bile-acid salts. *Kolloid.-Z. u. Z. Polymere* 244, 246-252.
- Green, A.L., 1967. Ionization constants and water solubilities of some aminoalkylphenothiazine tranquilizers and related compounds. *J Pharm Pharmacol.* 19, 10-16.
- Higuchi, T., Gupta, M., Busse, L.W., 1953. Influence of electrolytes, pH, and alcohol concentration on the solubilities of acidic drugs. *J. Amer. Pharm. Assoc. (Sci. Ed.)* 42, 157-161.
- Indulkar, A.S., Box, K.J., Taylor, R., Ruiz, R., Taylor, L.S., 2015. pH-Dependent liquid–liquid phase separation of highly supersaturated solutions of weakly basic drugs. *Mol. Pharmaceutics*, DOI: 10.1021/acs.molpharmaceut.5b00056.
- Jaszczyszyn, A., Gąsiorowski, K., Świątek, P., Malinka, W., Cieślik-Boczula, K., Petrus, J., Czarnik-Matusewicz, B., 2012. Chemical structure of phenothiazines and their biological activity. *Pharmacol. Reports* 64, 16-23.
- Jinno, J., Oh, D.-M., Crison, J.R., Amidon, G.L., 2000. Dissolution of ionizable water-insoluble drugs: the combined effect of pH and surfactant. *J. Pharm. Sci.* 89, 268-274.
- Ledwidge, M.T., Corrigan, O.I., 1998. Effects of surface active characteristics and solid state forms on the pH solubility profiles of drug-salt systems, *Int. J. Pharm.* 174, 187–200.
- Li, S., Wong, S., Sethia, S., Almoazen, H., Joshi, Y.M., Serajuddin, A.T.M., 2005a. Investigation of solubility and dissolution of a free base and two different salt forms as a function of pH. *Pharm. Res.* 22, 628-635.
- Li, S., Doyle, P., Metz, S., Royce, A.E., Serajuddin, A.T.M., 2005b. Effect of chloride ion on dissolution of different salt forms of haloperidol, a model basic drug. *J. Pharm. Sci.* 94, 2224-2231.
- Liu, S.-T., Hurwitz, A., 1977. The effect of micelle formation on solubility and pK_a determination of acetylpromazine maleate. *J. Colloid Int. Sci.* 60, 410-413.
- Mukerjee, P., Cardinal, J.R., 1976. Solubilization as a method for studying self-association: solubility of naphthalene in the bile salt sodium cholate and the complex pattern of its aggregation. *J. Pharm. Sci.* 65, 882-886.
- Ottaviani, G., Wendelspiess, S., Alvarez-Sánchez, R., 2015. Importance of critical micellar concentration for the prediction of solubility enhancement in biorelevant media. *Mol. Pharmaceutics* 12, 1171–1179.
- Patrick, G.L., 1995. *An Introduction to Medicinal Chemistry*. Oxford University Press, Oxford, UK.
- Pra Mauro, E., Pelezetti, E., 1996. *Surfactants in Analytical Chemistry – Applications of Organized*

Amphiphilic Media. Elsevier, Amsterdam.

- Roseman, T.J., Yalkowsky, S.H., 1973. Physical properties of prostaglandin F2 α (tromethamine salt): solubility behavior, surface properties, and ionization constants. *J. Pharm. Sci.* 62, 1680-1685.
- Serajuddin, A.T.M., Rosoff, M, 1984. pH-solubility profile of papaverine hydrochloride and its relationship to the dissolution rate of sustained-release pellets. *J. Pharm. Sci.* 73, 1203-1208.
- Serajuddin, A.T.M., Jarowski, C.I., 1985. Effect of diffusion layer pH and solubility on the dissolution rate of pharmaceutical bases and their hydrochloride salts. I: phenazopyridine. *J. Pharm. Sci.* 74, 142-147.
- Serajuddin, A.T.M., Mufson, D., 1985. pH-Solubility profiles of organic bases and their hydrochloride salts. *Pharm. Res.* 1985, 2, 65-68.
- Shalaeva, M., Kenseth, J., Lombardo, F., Bastin, A., 2008. Measurement of dissociation constants (pK_a values) of organic compounds by multiplexed capillary electrophoresis using aqueous and cosolvent buffers. *J. Pharm. Sci.* 97, 2581-2606.
- Shoghi, E., Fuguet, E., Bosch, E., Rafols, C, 2012. Solubility-pH profile of some acidic, basic and amphoteric drugs. *Eur. J. Pharm. Sci.* 48, 290-300.
- Sorby, D.L., Plein E.M., Benmaman, J.D., 1966. Adsorption of phenothiazine derivatives by solid adsorbents. *J. Pharm. Sci.* 55, 785-794.
- Stokes, R.H., Robinson, R.A., 1948. Ionic hydration and single ion activities in unassociated chlorides at high ionic strengths. *J. Amer. Chem. Soc.* 70, 1870-1878.
- Streng, W.H., 1999. The Gibbs constant and pH solubility profiles. *Int. J. Pharm.* 186, 137-140.
- Sun, N., Avdeef, A., 2011. Biorelevant pK_a (37°C) Predicted from the 2D Structure of the Molecule and its pK_a at 25°C. *J. Pharm. Biomed. Anal.* 56, 173-182.
- Takács-Novák, K., Tam, K.Y., 2001. Multiwavelength spectrophotometric determination of acid dissociation constants: a validation study. *Anal Chim Act.* 434,157–167.
- Tsinman, O., Tsinman, K., Sun, N., Avdeef, A., 2011. Physicochemical selectivity of the BBB microenvironment governing passive diffusion – matching with a porcine brain lipid extract artificial membrane permeability model. *Pharm. Res.* 28, 337-363.
- Völgyi, G., Ruiz, R., Box, K., Comer, J., Bosch, E., Takács-Novák, K., 2007. Potentiometric pK_a determination of water-insoluble compounds: validation study in a new cosolvent system. *Anal. Chim. Acta* 583, 418-428.
- Völgyi, G., Marosi, A., Takács-Novák, K., Avdeef, A., 2013. Salt Solubility Products of Diprenorphine Hydrochloride, Codeine and Lidocaine Hydrochlorides and Phosphates – Novel Method of Data Analysis Not Dependent on Explicit Solubility Equations. *ADMET & DMPK* 1, 48-62.
- Wang, Z., Burrell, L.S., Lambert, W.J., 2002. Solubility of E2050 at various pH: a case in which the apparent solubility is affected by the amount of excess solid. *J. Pharm. Sci.* 91, 1445-1455.

- Wohlfarth, C., 2008. Lechner M.D. (ed.) SpringerMaterials. Dielectric constant of the mixture (1) water; (2) propan-1-ol Landolt-Börnstein - Group IV Physical Chemistry 17 (Supplement to IV/6).
- Zhu, C., Streng, W.H., 1996. Investigation of drug self-association in aqueous solution using calorimetry, conductivity, and osmometry. *Int. J. Pharm.* 130, 159-168.
- Zografi, G., Zarenda, I., 1966. The surface activity of phenothiazine derivatives at the air-solution interface. *Biochem. Pharmacol.* 15, 591-598.
- Zografi, G., Auslander, D.E., Lytell, P.L., 1964. Interfacial properties of phenothiazine derivatives. *J. Pharm. Sci.* 53, 573-574.

Table 1 - Conditions during chromatographic separation ^a

Compound	A(%)	B(%)	Flow Rate (mL·min⁻¹)	λ(nm)
Promazine.HCl	70	30	1	245
Chlorpromazine.HCl	70	30	1	255
Triflupromazine.HCl	75	25	1	250
Perphenazine	70	30	1	255
Fluphenazine.2HCl	65	35	1	255
Trifluoperazine.2HCl	75	25	1	255

^a Mobile phases: A = methanol, B = pH 7 phosphate buffer.

Table 2 - Ionization constants (pK_a) of phenothiazine derivatives at 25 and 37 °C ^a

Compound	pK_a	t (°C)	Ionic Str. (M)	Cosolvent Range	Weighted Fit Slope ^a	Ref
Promazine.HCl	9.63 ± 0.10 ^b	25	0.15 ^b	30-60 wt% MeOH	-0.0205	Shalaeva <i>et al.</i> , 2008
	9.11 ± 0.03	37	0.16	15-33 wt% n-PrOH	-0.0486	this work
Chlorpromazine.HCl	9.57 ± 0.02 ^c	25	0.15 ^g	30-60 wt% MeOH	-0.0240	Avdeef, 1994, 2001; Shalaeva <i>et al.</i> , 2008
	8.70 ± 0.03	37	0.16	15-33 wt% n-PrOH	-0.0413	this work
Triflupromazine.HCl	9.47 ± 0.01 ^d	25	0.15	5-64 wt% MeOH ^d	-0.0246	this work
	8.65 ± 0.02	37	0.16	15-33 wt% n-PrOH	-0.0438	this work
Fluphenazine.2HCl	7.84 ± 0.02 ^e	25	0.18	20-39 wt% MeOH	-0.0094	Tsinman <i>et al.</i> , 2011
	3.98 ± 0.03 ^e	25	0.18	20-39 wt% MeOH	-0.0157	Tsinman <i>et al.</i> , 2011
	7.51 ± 0.03	37	0.16	15-33 wt% n-PrOH	-0.0274	this work
	3.37 ± 0.04	37	0.16	0-33 wt% n-PrOH	-0.0293	this work
Perphenazine	7.95 ± 0.04	25	0.19	12-39 wt% MeOH	-0.0085	Tsinman <i>et al.</i> , 2011
	3.66 ± 0.10	25	0.19	12-39 wt% MeOH	-0.0235	Tsinman <i>et al.</i> , 2011
	7.64 ± 0.02	37	0.16	15-33 wt% n-PrOH	-0.0303	this work
	3.42 ± 0.04	37	0.16	0-33 wt% n-PrOH	-0.0214	this work
Trifluoperazine.2HCl	8.43 ± 0.17	25	0.17	26-48 wt% MeOH	-0.0167	Tsinman <i>et al.</i> , 2011
	4.85 ± 0.85 ^f	25	0.17	26-48 wt% MeOH	-0.0603	Tsinman <i>et al.</i> , 2011
	7.92 ± 0.06	37	0.15	15-33 wt% n-PrOH	-0.0332	this work
	3.70 ± 0.03	37	0.15	0-33 wt% n-PrOH	-0.0387	this work

^a The individual apparent pK_a values as a function of % cosolvent were extrapolated to zero cosolvent, using weighted linear regression. Cosolvent potentiometric data were used, except as noted.

^b Cosolvent capillary electrophoresis data ($I = 0.05$ M), with extrapolated $pK_a = 9.62$. Value was then adjusted to $I = 0.15$ M basis.

^c Combined cosolvent potentiometric ($I = 0.16$ M) and capillary electrophoresis data ($I = 0.05$ M). Final pK_a is reported with reference to $I = 0.15$ M.

^d Combined cosolvent potentiometric (34-64 wt% MeOH) and spectrophotometric (5-52 wt% MeOH) data.

^e With the 2- pK_a piperazine derivatives, the higher value refers to pK_{a2} and the lower value (italic) refers to pK_{a1} .

^f The high error may be indicative of precipitation of the doubly-charged drug in methanol-rich solutions.

^g The actual average ionic strength in the combined CE and potentiometric data was $I = 0.11$ M. The pK_a was essentially unchanged at $I = 0.15$ M.

FIGURE CAPTIONS

Fig. 1 - Chemical structures of the six phenothiazine derivatives.

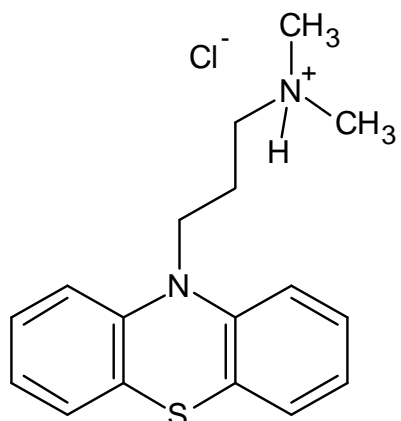
Fig. 2 – Weighted linear regression plots, $p_s K_a$ vs. wt% cosolvent, of the phenothiazine derivatives at 25 °C (MeOH/H₂O) and 37 °C (*n*-PrOH/H₂O). Most of the data are based on potentiometric determinations, with the following exceptions. The promazine plot at 25 °C (Fig. 2a) is based on CE data (Shalaeva *et al.*, 2008). For chlorpromazine at 25 °C (Fig. 2c), the square symbols denote CE determinations (Shalaeva *et al.*, 2008), whereas the circles correspond to potentiometric data (Avdeef, 1994, 2001). For triflupromazine at 25 °C (Fig. 2e), the unfilled circles are based on spectrophotometric data, while the filled circles are from potentiometric determinations. Table 2 summarizes the results of the pK_a analysis.

Fig. 3 – Solubility-pH profiles for the phenothiazine derivatives at 25 and 37 °C, adjusted to the reference ionic strengths 0.15-0.19 M, the mean values from the pK_a determinations (see text). The dashed curves were calculated with the Henderson-Hasselbalch equation, using the pK_a and S_0 constants (Tables 2 and 3). The solid lines are best-fit refinement curves through the measured log S-pH points. The dash-dot curves below pH 7 were calculated from the predicted solubility products, using Eqs. (10) and (11). There was evidence of precipitation of the 2:1 drug-phosphate salt for promazine (both temperatures) and triflupromazine (37 °C). The dotted lines (Figs. 3k,l) indicate that the compound is predicted to completely dissolve even in 1 M solutions (see text). The black-circle-with-cross-at-the-center symbols in the 2- pK_a drug plots (g-l) indicate the pH points corresponding to the two pK_a values. The details of the calculations are summarized in Table 3.

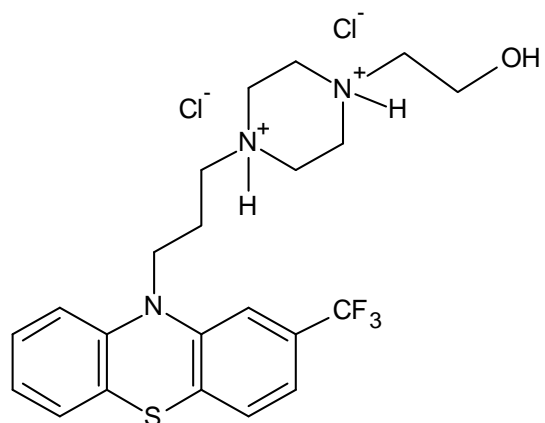
Fig. 4 - Differential scanning calorimetry (DSC) thermograms of the phenothiazine derivatives, taken of the original solids (dotted curves), the solids isolated from pH 7 suspensions (dashed curves) and pH 10 suspensions (solid curves).

Fig. 5 – Comparison of intrinsic solubility of phenothiazines to averaged values taken from the

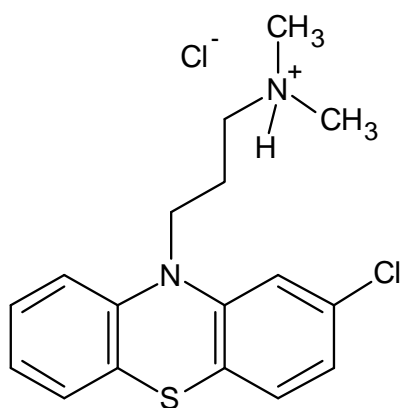
literature. The literature results are summarized in Table 5 and are at 25 °C (except fluphenazine, which is at 37 °C).



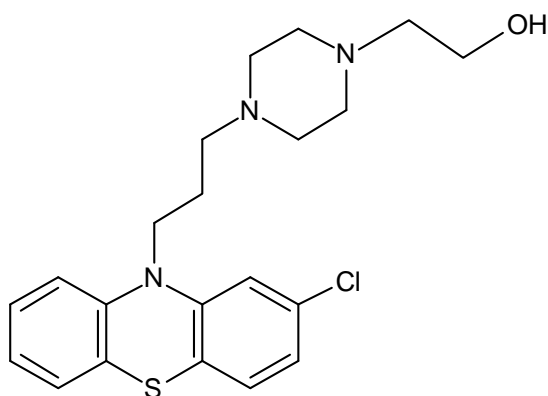
Promazine.HCl



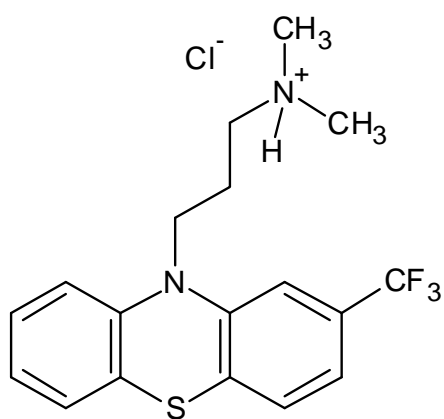
Fluphenazine.2HCl



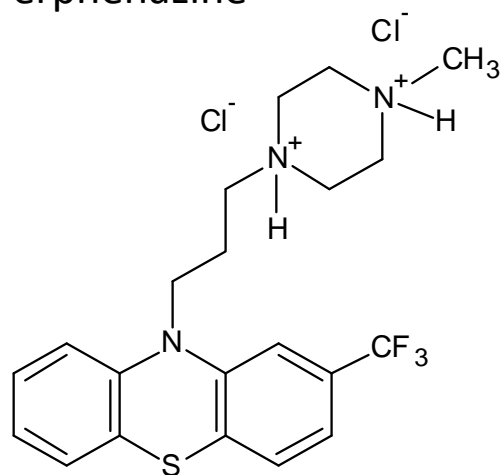
Chlorpromazine.HCl



Perphenazine



Triflupromazine.HCl



Trifluoperazine.2HCl

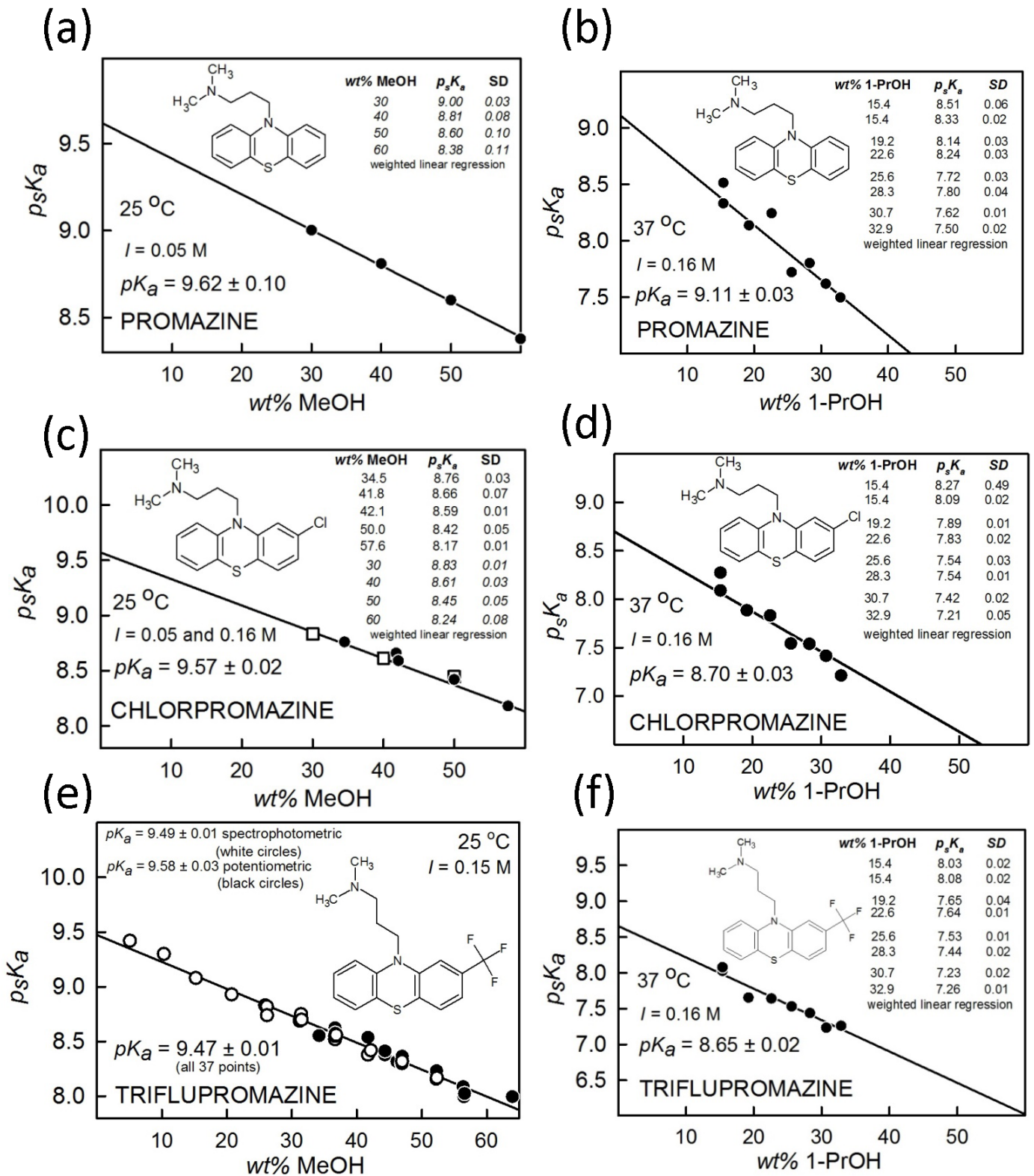


Fig. 2 – Pobudkowska et al.

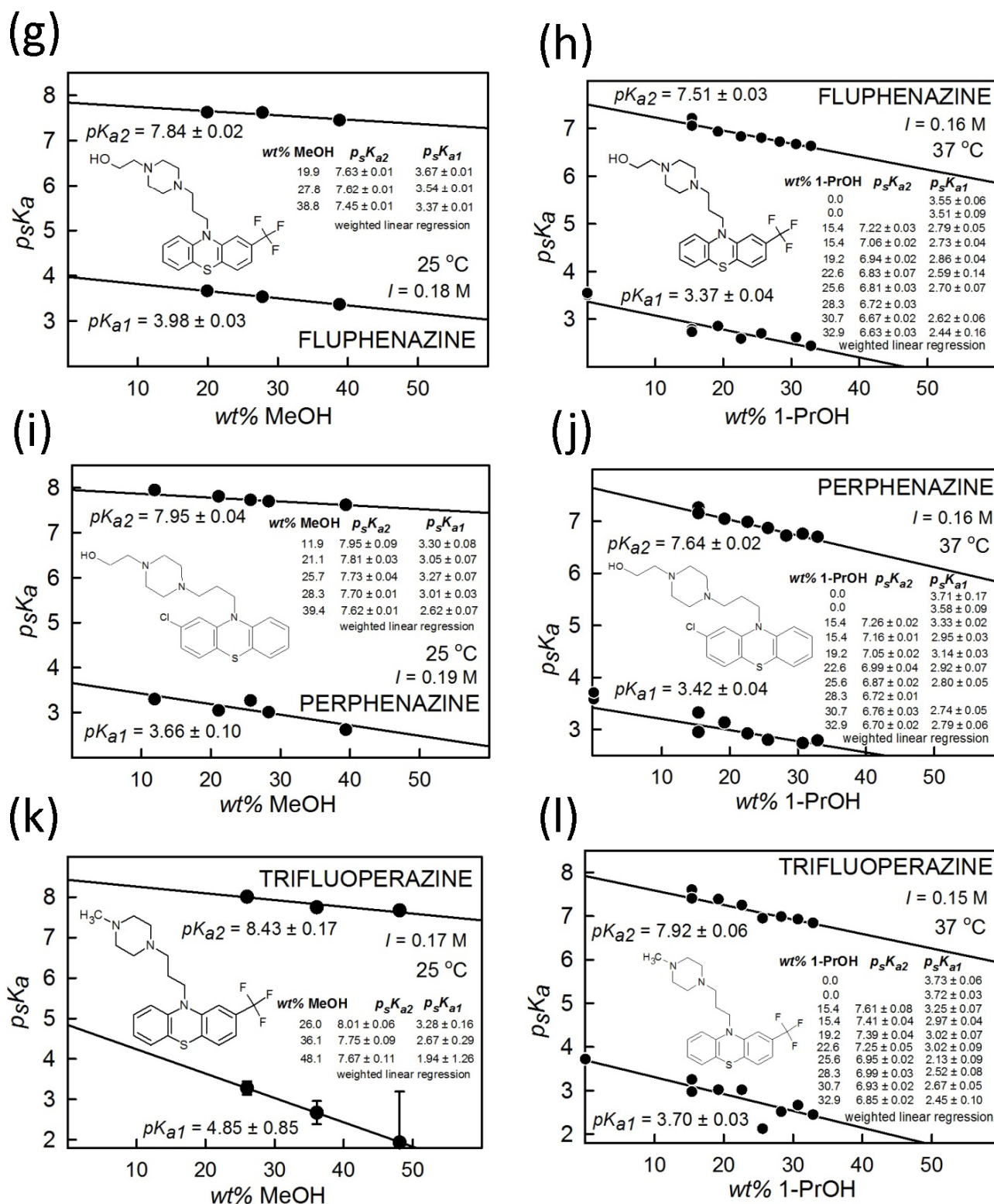


Fig. 2 – Pobudkowska et al.

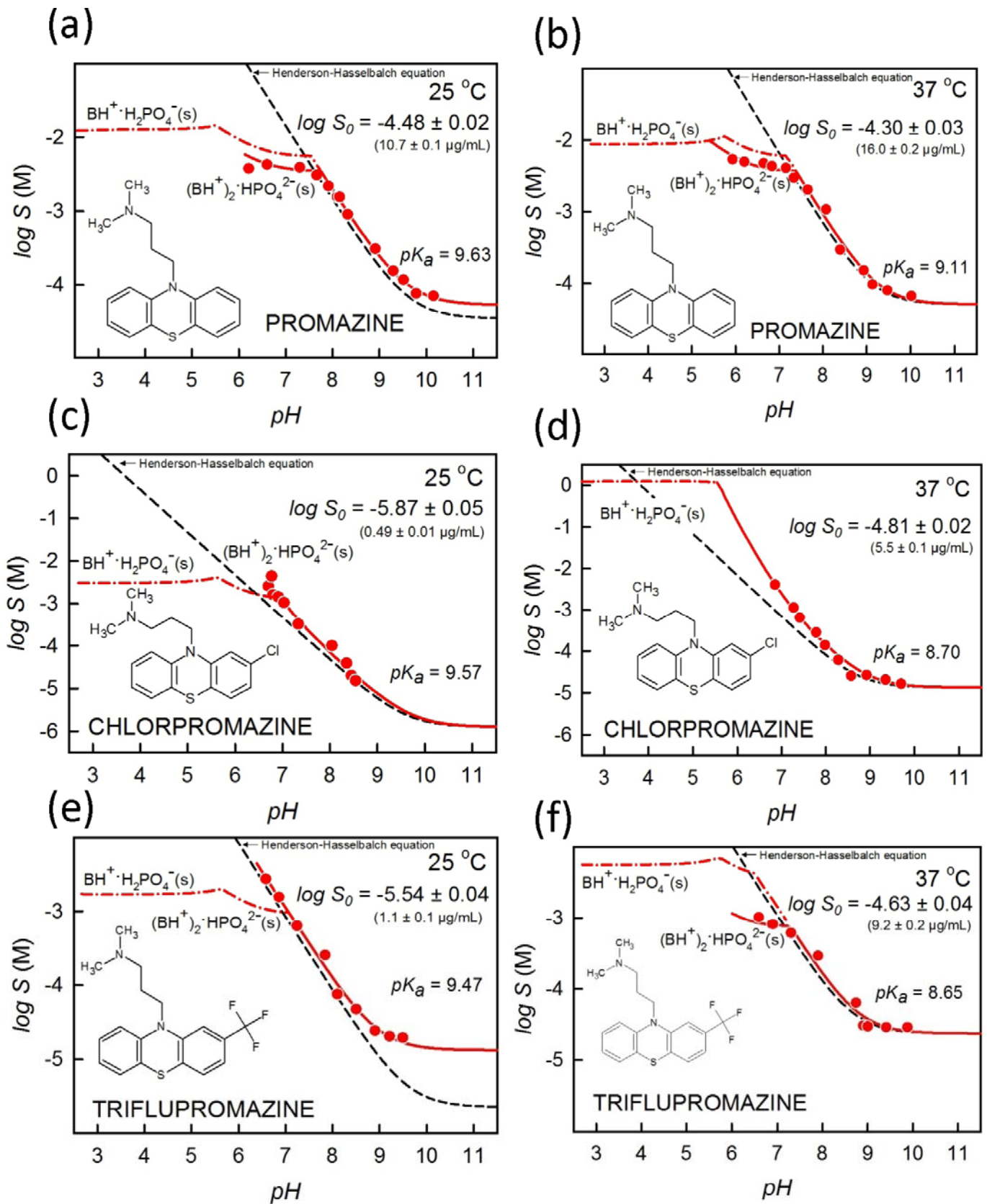


Fig. 3 – Pobudkowska et al.

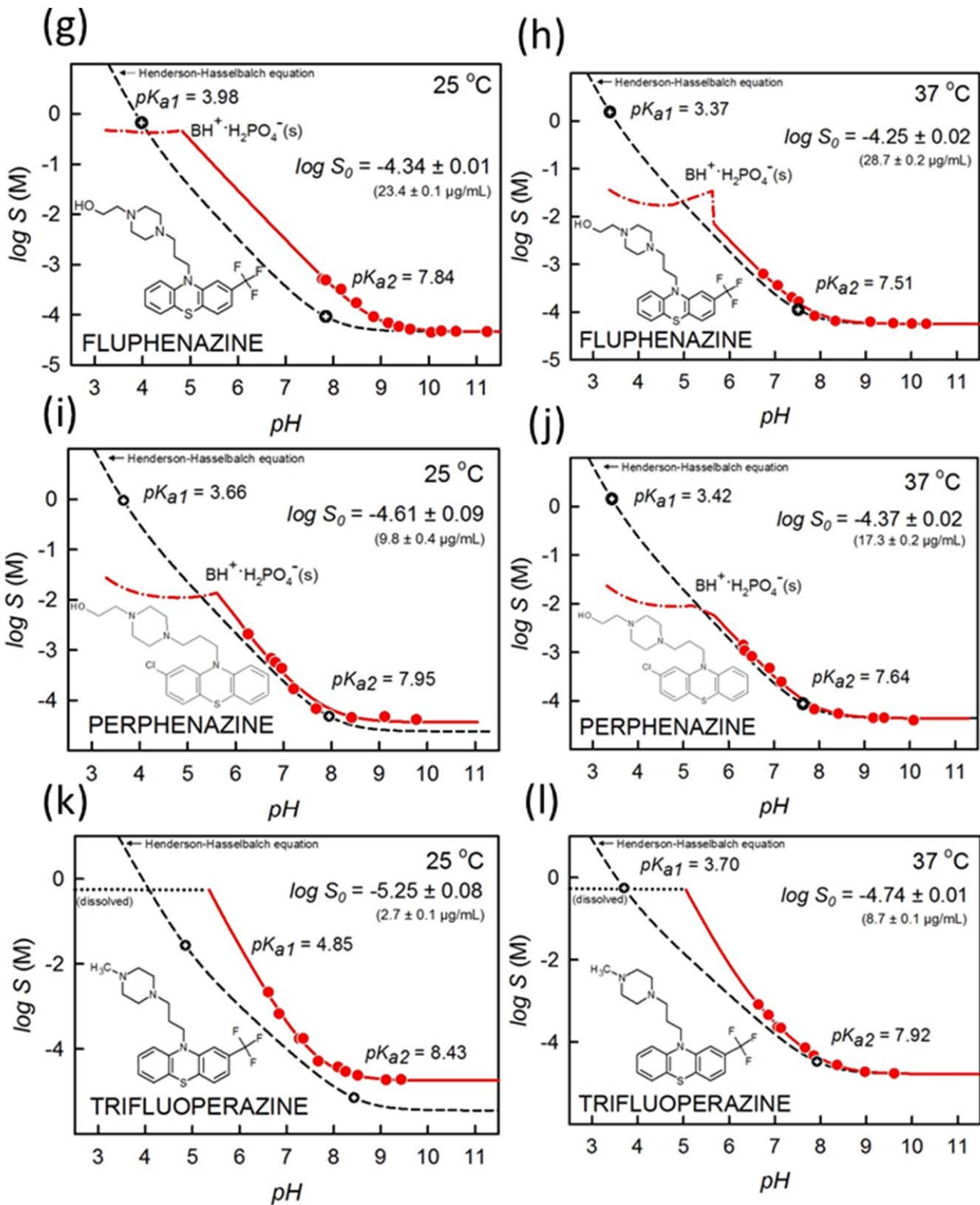


Fig. 3 – Pobudkowska et al.

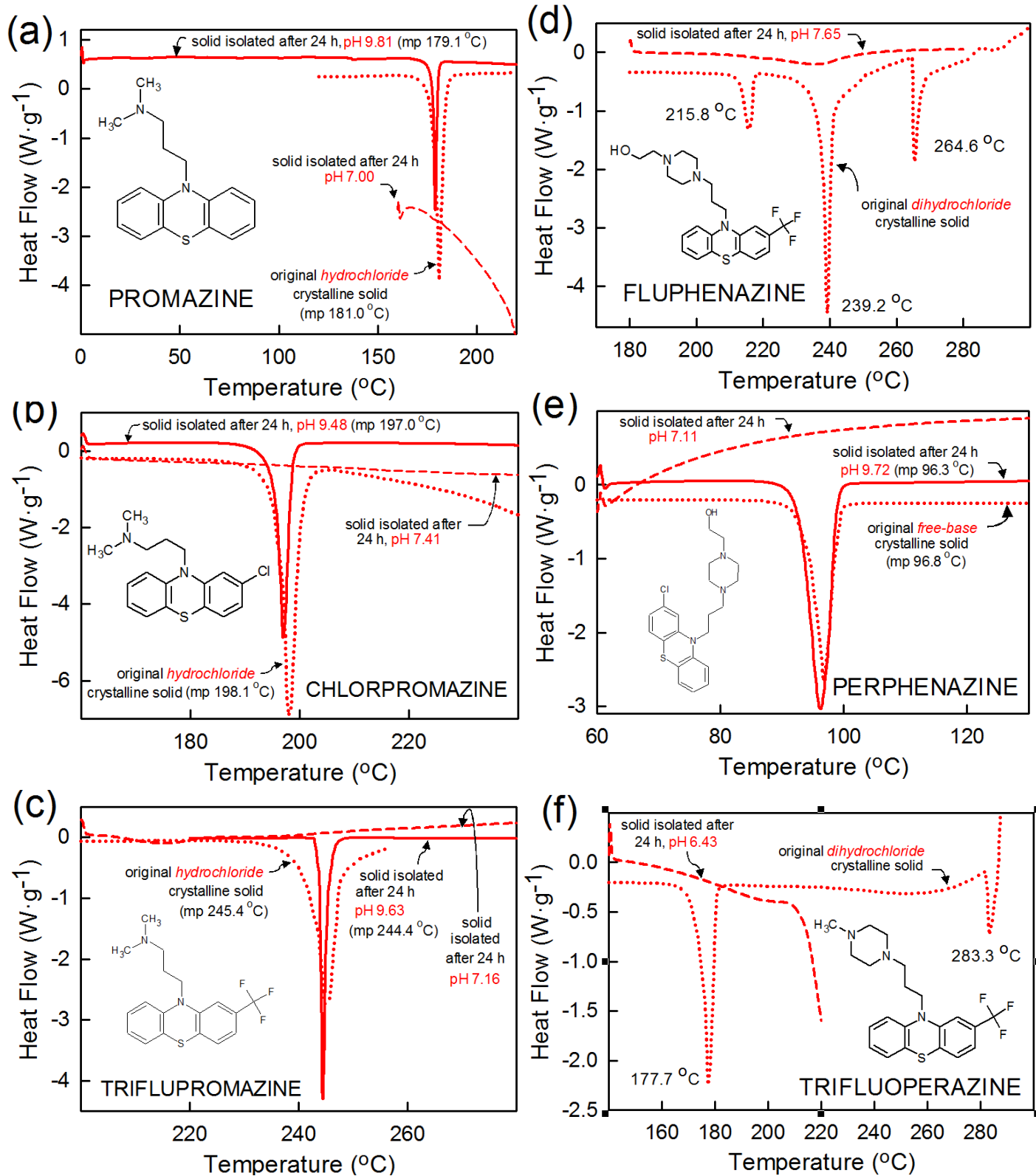


Fig. 4 – Pobudkowska et al.

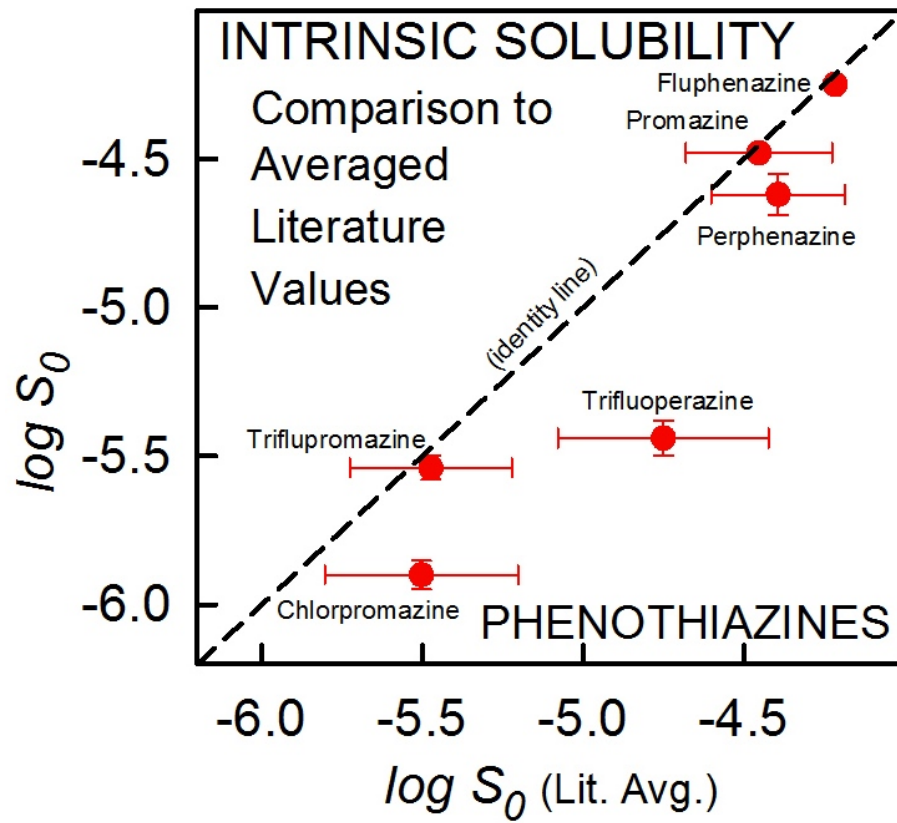


Fig. 5 – Pobudkowska et al.